Bulgarian Chemical Communications, Volume 54, Issue 4 (pp. 310-317) 2022 *DOI: 10.34049/bcc.54.4.5485*

Minimization of free energy in dye removal from an aqueous solution by a biosorbent *Ricinus communis* using response surface technology

V. K. Sohpal

Department of Chemical Engineering & Bio Technology, SBS State University, Gurdaspur 143521, Punjab, India

Received: April 04, 2022; Accepted: September 22, 2022

The present work focuses on applying response surface methodology (RSM) for the minimization of Gibbs free energy for crystal violet dye (CVD) removal from a solution by a bioadsorbent *Ricinus communis*. Central composite design (CCD) and response surface methodology were used to conduct and analyze the experiments. The minimization of free energy was investigated as a function of three process variables, temperature (27-57 ^{o}C), absorbance (0.08-0.15 a.u.), and dye concentration (0.5-0.9 mg/l) with a fixed stirrer speed (120 rpm). The minimization of Gibbs free energy in the adsorption process was estimated by optimizing capacity of adsorption, percentage of dye removal, and temperature. The optimum values of percentage of removal of dye, adsorption capacity, and free energy were found to be 93.38 %, 0.965 mg/g, -8202.7 J/mol at temperature 55.9°C, respectively, having desirability > 95% for removal of crystal violet dye. The experimental observations were in good agreement with the predicted values.

Keywords: Response surface methodology; temperature; optimization; *Ricinus communis*; Gibbs free energy and minimization.

INTRODUCTION

The Asian textile industries consume large quantities of dyeing material and produce substantial amounts of colored wastewater. Different chemical techniques are used to remove various types of dyes to reduce water pollution. Adsorption is a prominent way to reduce water pollution with biomaterial and synthetic material. CuS nanoparticles loaded on activated carbon composite assist in removing indigo carmine and safranin-O [1]. RSM and ANN approach were used to optimize dye removal by adsorption, and results indicate 52.0% simulated behavior analogous to experimental work [2]. 3D graphene aerogel/ $CaCO_3$ nanocomposite absorbent were used to remove acid red (88) dye from aqueous solutions and RSM showed the optimized process parameters to remove 100% dye in fixed criteria [3]. Protein-rich solution with aluminum-based nanosheets was synthesized to remove congo red and crystal violet, and RSM observed with the optimum adsorbent dosages was 0.16 g for 50 mg/L, and 0.12 g for 100 mg/L for CR and CV dye solutions, respectively [4]. RSM was used to maximize the percent gel fraction to the removal of rhodamine-B (70%) and auramine-O (63%) from a mixture with an adsorbent dose of 700 mg [5]. ANN and RSM were applied to analyze the fixed bed adsorption of FD&C red 40 dye on polyurethane/chitosan foam and found that ANN can predict the experimental data with more accuracy than the RSM [6]. Chitosan cross-linked with graphene oxide was used to remove the dye safranin orange, and optimum parameters predicted using the RSM model are pH 6.82, initial SO concentration 425 mg/L [7]. Nanocomposite hydrogel from nano bismuth iron oxide synergistically coupled network of acrylic acid and RSM techniques was applied to optimize the kinetic variables [8]. Scrutinized were the different physicochemical processes using RSM in dye removal and some suggestions were made for future work on adsorption, advanced oxidation processes, coagulation/flocculation, and electro-coagulation [9]. Ni-doped ferric oxy-hydroxide FeO (OH) nanowires were synthesized for removal of safranin-O and indigo carmine and adsorption performance was analyzed using RSM, ANN, and linear algebra-based models [10]. Box–Behnken design was used to optimize the efficiency of amine-functioned Fe_3O_4 magnetic nanoparticles for removing RB5 azo dye from an aqueous solution [11]. Coagulants were used to achieve the optimum conditions for the removal of color and turbidity using a biopolymer with the RSM design and it was observed that at optimum conditions the removal of color and turbidity was 76.20% and 90.14%, respectively [12].

The nanocomposite of $MnFe_2O_4$ synthesized for its application as an adsorbent for direct red 16 (D R16) removal and central composite rotatable design (CCRD) combined with RSM was used to optimize the adsorption capacity [13]. Graphene oxide nano-platelets were used for simultaneous adsorption of acid yellow 36 (AY) and acid blue 74 (AB) and

* To whom all correspondence should be sent:
E-mail: vipan752002@gmail.com

process parameters were optimized for best results using RSM and ANN [14]. RSM has been applied to determine the optimal adsorbent composition and experimental conditions for the removal of basic violet and malachite green oxalate dyes using activated phosphorus slag-based cylindrical adsorbent [15]. RSM was utilized to simulate and determine the optimum conditions of RB19 removal by functionalized MWCNTs using adsorbent dose, initial dye concentration, and pH and R^2-value of 89.11% and adjusted R^2-value of 95.72% were obtained [16]. RSM-CCD techniques were used to optimize the synthesis scheme of semi-IPN nanocomposite adsorbent for removing biebrich scarlet and crystal violet. Results suggested the recyclability and reusability of the adsorbent materials for the textile industry [17]. RSM and ANN modeling were used to remove Pb (II) by thiosemicarbazide-modified chitosan, and the desirability degree for the RSM optimization predicted was 0.981 [18]. Iron zero-valent nanoparticles were synthesized for removal of methylene blue dye in water solution. CCD was applied to optimize the removal of dye and R^2 and adj. R^2 correlation coefficients for the model observed were 0.96 and 0.93, respectively [19]. RSM method was used to optimize the palm oil for caffeine adsorption and observed that removal efficiency (%) at the optimal conditions, 0.20 g of adsorbent, initial caffeine concentration of 20 mg/L, and acidic medium was about 95% [20]. RSM-BBD was employed to optimize the MO dye removal efficiency from aqueous solution by cross-linked Chi-TPP/NTC). The F-value for MO removal efficiency was 93.4 (corresponding p-value < 0.0001) [21]. Shoes waste adsorbents with CCD techniques were applied to investigate the removal of cadmium (Cd) from aqueous solution and wastewater. The result confirms CCD as the best statistical model to predict the response with good accuracy and reliability [22].

Adsorption isotherms and kinetic models investigated the use of *Ricinus communis* as a natural adsorbent for removing dyes from aqueous solution and the natural adsorbent was found viable at an economical cost [23]. The present study focused on *Ricinus communis* as a natural adsorbent for CV dye removal using RSM and CCD statistical techniques. The RSM with CCD was used to develop a mathematical model to predict the desirability parameter using an optimized correlation between maximum adsorption capacity, minimization of free energy, and a higher percentage of dye removal.

MATERIALS AND METHODS

In this study, CVD (IUPAC: Tris (4-(dimethylamino) phenyl) methylium chloride) was used to prepare synthetic dye wastewater. This dye was obtained from Loba Chemicals, Mumbai, India. Analytical grade (80% purity) CVD was used without purification to prepare the stock solution (1000 mg/l) by dissolving a precise quantity of dye in distilled water. *Ricinus communis* leaves were subjected to physical (washing, boiling, and soaking) and chemical (drying) treatment and finally the dried leaves were crushed to a particle size of about 53 µm. The maximum absorbance wavelength (λ_{max}) for CVD was found to be 585 nm.

Batch adsorption investigations were performed to evaluate the effect of various process variables on the dye removal percentage, adsorption capacity, and Gibbs free energy. All the batch adsorption experiments were conducted according to the CCD matrix at random to reduce the possibility of errors. In addition, minimum and maximum levels of each of the three input process variables [temperature (27-57°C), absorbance (0.08-0.15 a.u.), and dye concentration (0.5-0.9 mg/L) with a fixed stirrer speed (120 rpm)] were evaluated through pre-trial experiments [23].

RESULTS AND DISCUSSION

Effect of temperature on free energy

The temperature-dependent thermodynamic variable changes in the Gibbs free energy (ΔG°), enthalpy (ΔH°), and entropy (ΔS°) of the adsorption process were estimated using the correlation $\Delta G^o = \Delta H^o - T\Delta S^o$.

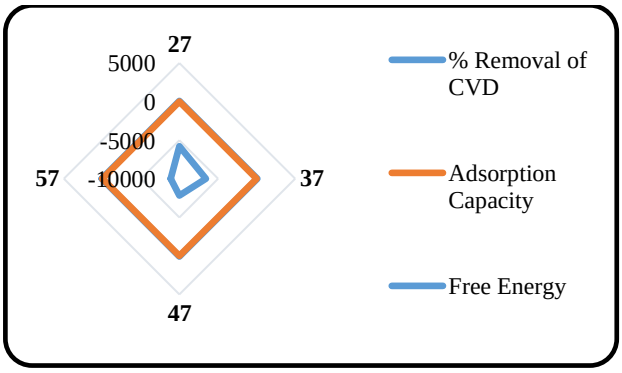

Fig. 1. Temperature *vs.* adsorption capacity, free energy and % removal of CVD

A plot of ΔG° *versus* T yields a straight line with the slope of –ΔS° and intercept of ΔH°. The values of ΔG° obtained using different temperatures of the reaction are shown in Fig. 1. The ΔH° and ΔS° values during the adsorption process determined from the slope and intercept are 25670 J/mol and

104.2 J/mol, respectively, for CVD. The positive values indicate that the adsorption process is endothermic in nature, and forward reactions are favored.

Central composite design for experimental work

CCD was applied to assess the optimum operating parameters for CVD removal using Design operating Expert software. In this study, the three independent variables investigated for the removal of CVD, adsorption capacity and free energy were t, temperature (27-57^{o}C), a, absorbance (0.08-0.15 a.u.), and c, concentration of dye (0.5-0.9 mg/L). The responses of the percent removal of CVD, adsorption capacity (mg/g), and Gibbs free energy (J/mol) using CCD are represented in Table 1.

Table 1. Full factorial CCD matrix for CVD removal absorption process

Run order using CCD			Temperature (t, ^{o}C)	Absorbance (a)	Conc. of dye (c)	% Removal of dye	Adsorption Capacity	Free Energy
19	2	Center	47	0.115	0.7	93.88	0.945	-7001.1
17	4	Center	47	0.115	0.7	93.87	0.945	-7001.1
15	5	Center	47	0.115	0.7	93.88	0.946	-7001.6
20	8	Center	47	0.115	0.7	93.89	0.945	-7001.8
16	11	Center	47	0.115	0.7	93.88	0.948	-7001.2
18	17	Center	47	0.115	0.7	93.88	0.945	-7001.1
14	6	Axial	47	0.115	0.9	90.04	0.918	-6992.01
10	7	Axial	57	0.115	0.7	93.04	0.963	7793.01
9	14	Axial	27	0.115	0.7	91.04	0.910	-5783.01
11	15	Axial	47	0.08	0.7	93.95	0.962	-7695.13
13	16	Axial	47	0.115	0.5	93.22	0.961	-7692.15
12	20	Axial	47	0.15	0.7	92.95	0.95	-7700.13
3	1	Fact	37	0.15	0.5	91.22	0.923	-6980.2
6	3	Fact	57	0.08	0.9	92.55	0.921	-8870
4	9	Fact	57	0.15	0.5	91.04	0.91	-8859
1	10	Fact	37	0.08	0.5	92.22	0.922	-6950
8	12	Fact	57	0.15	0.9	92.04	0.92	-8872
2	13	Fact	57	0.08	0.5	92.53	0.93	-8850
5	18	Fact	37	0.08	0.9	91.05	0.91	-6977
7	19	Fact	37	0.15	0.9	91.04	0.914	-6970

RSM modeling for percentage removal of dye

Statistically designed experiments using CCD were performed to study the effect of the independent variables on the percent removal of dye. The design matrix corresponding to predicted results is shown in Table 1. A 2nd order polynomial model was developed using the observed data in terms of coded factors (t, a, c) employing RSM as given in eq. (1):

$$\text{Percent removal of dye} = 62.66 + 0.76 \times t + 47.23 \times b + 30.24 \times c - 0.60t \times b + 0.096t \times c - 0.007 \times t^2 - 136.73 \times b^2 - 25.66 \times c^2 \quad (1)$$

ANOVA results presented in Table 2 were used to evaluate the model. Coefficients of the model were estimated using regression analysis, and the R-squared coefficient was evaluated for judgment of fitness of the model. As a result, the model was established to be significant and applicable to track the design domain. Fisher test (F) statistical technique significance on the model was also analyzed. A small p-value compared to F showed that the quadratic model developed was statistically significant and used to predict the percentage of dye removal.

Temperature, absorbance, and concentration of CVD are essential parameters for the adsorption

process. Fig. 2(a) shows a three-dimensional relationship between the temperature and absorbance concerning the percentage of CVD removal. The percentage of CVD removal increases from 91% to 96% as the solution temperature increases from 27 to 57°C. Because the adsorption increased as the temperature increased, the system is considered to be endothermic. On the same temperature trend, the absorbance declines up to 5% due to that CVD removal percentage.

From the RSM surface plot, it is clear that at 47°C with absorbance 0.115 a.u. 93.89% of CVD is removed which is close to the experimental result of 94.70%. Fig. 2(b) shows a three-dimensional relationship between the temperature and concentration of CVD concerning the percentage of CVD removal. Due to the endothermic chemisorption process, the lower concentration of dye improves the CVD removal percentage. As the temperature rises, the bonding of dye and active sites of the adsorbent weakened. A virtue of that interaction between the solute and solvent becomes stronger. In addition, dye solubility also increased at elevated temperature. RSM surface plot obviously reflects that at 47°C with dye concentration 0.7 mg/L 93.89% of CVD is removed, close to the experimental result. The variation between experimental and ANOVA predicted result for % CVD removal is less than 1% due to R^2 0.9891, Adj. $R^2 = 0.9813$, Pred. $R^2 = 0.9585$.

Table 2. ANOVA for response surface reduced quadratic model for percentage removal of dye

Source	Sum of Squares	df	Mean Square	F Value	p-Value Prob. > F	Percent Contribution	Remarks
Model	27.317	8	3.415	125.32	< 0.0001		Significant
t	1.339	1	1.339	49.143	< 0.0001	5.11	
b	2.7197	1	2.72	99.815	< 0.0001	9.81	
c	0.7362	1	0.736	27.02	0.0003	2.64	
t×*b*	0.3612	1	0.361	13.258	0.0039	1.30	
t×*c*	0.2965	1	0.296	10.88	0.0071	1.05	
t^2	8.7486	1	8.749	321.08	< 0.0001	31.66	
b^2	0.4043	1	0.404	14.839	0.0027	1.44	
c^2	15.189	1	15.19	557.45	< 0.0001	54.98	
Residual	0.2997	11	0.027			1.08	
Lack of Fit	0.1722	6	0.029	1.1251	0.4583		Not significant
Pure Error	0.1275	5	0.026				
Cor Total	27.617	19					

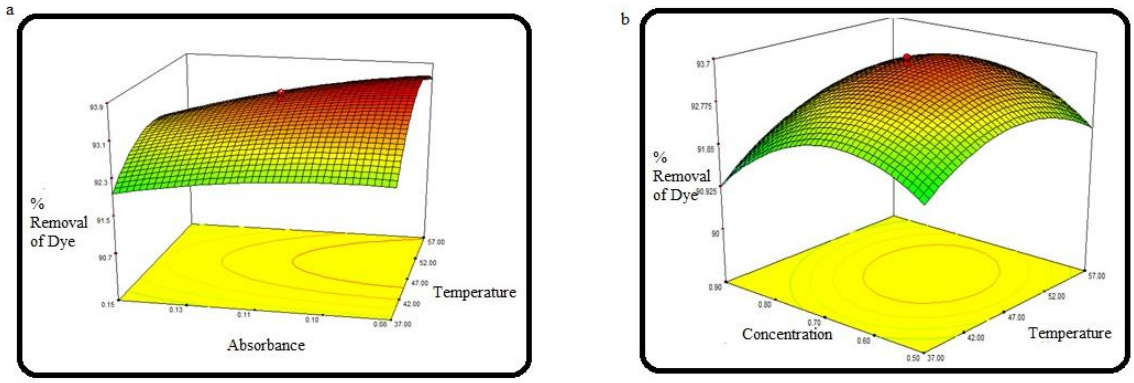

Fig. 2 (a) Surface plots of percent removal of dye with respect to temperature and absorbance; (b) Surface plots of percent removal of dye with respect to temperature and concentration of dye.

RSM modeling for adsorption capacity

CCD was performed to investigate the effect of the independent variables on adsorption capacity. Table 1 represents the design matrix and corresponding predicted results. A polynomial model was developed for adsorption capacity using RSM as given in eq. (2):

$$\text{Adsorption capacity} = 0.62 + 0.013 \times t - 0.88 \times b + 0.19 \times c - 0.00075 \times t \times c + 1.21 \times b \times c - 0.00013\, t^2 - 0.314\, b^2 - 0.257\, c^2 \quad (2)$$

ANOVA results presented in Table 3 were used to evaluate the model. Fig. 3(a) shows a three-dimensional relationship between the temperature and concentration of dye for absorption capacity. The adsorption capacity increases from 0.910 to 09.68 as temperature increases from 27 to 57°C. The adsorption capacity of the adsorbate increased as the temperature increased due to endothermic effect. From RSM surface plot it is clear that at 57°C with a concentration of dye 0.7 mg/L the adsorption capacity is 0.962, close to the experimental result 0.953. Fig. 3 (b) shows a three-dimensional relationship between the absorbance and concentration of CVD for adsorption capacity. The adsorption capacity increases with the higher initial concentration of dye from 0.5 mg/L to 0.7 mg/L at maximum temperature 57°C, and the sorption capacity increased from 0.71 to 0.9 mg/L. In contrast, the removal percentage of dye decreased from 93% to 91%. The variation between experimental and ANOVA predicted result for adsorption capacity is lower than 1% due to R^2 0.9881. Adj. R^2= 0.9795, Pred. R^2 = 0.9574.

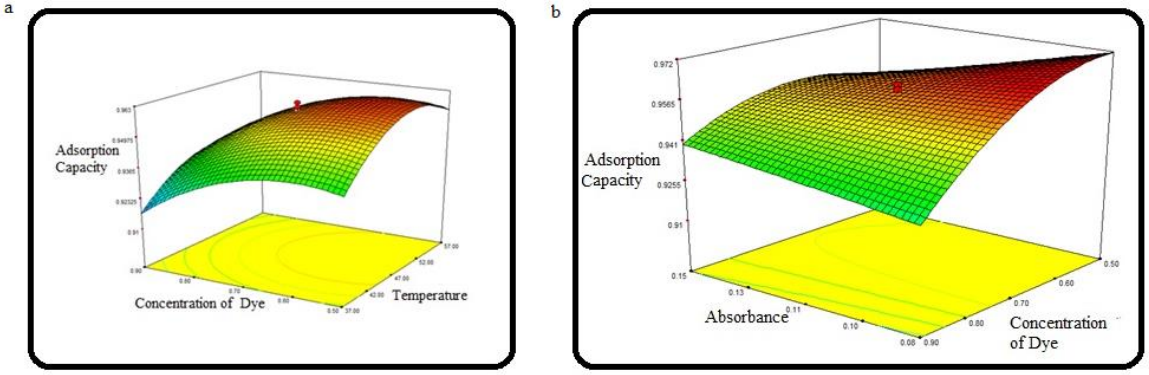

Fig. 3. (a) Surface plots of adsorption capacity with respect to temperature and concentration of dye; (b) Surface plots of adsorption capacity with respect to absorbance and concentration of dye.

Table 3. ANOVA for response surface reduced quadratic model adsorption capacity

Source	Sum of Squares	df	Mean Square	F Value	p-Value Prob. > F	Percent Contribution	Remarks
Model	0.0072	8	0.0009	114.31		< 0.0001	Significant
t	0.0006	1	0.0006	77.38	8.57	< 0.0001	
b	0.0001	1	0.0001	22.48	1.42	0.0006	
c	0.002	1	0.002	254.46	28.57	< 0.0001	
t×c	0.000017	1	0.000017	2.28	0.24	0.1591	
b×c	0.0005	1	0.0005	73.25	7.14	< 0.0001	
t^2	0.0026	1	0.0026	331.24	37.14	< 0.0001	
b^2	0.0000021	1	0.0000021	0.27	0.02	0.6128	
c^2	0.0015	1	0.0015	193.20	21.42	< 0.0001	
Residual	0.000086	11	0.0000078		1.22		
Lack of Fit	0.00005	6	0.0000084	1.17		0.4389	Not significant
Pure Error	0.00003	5	0.0000072				
Cor Total	0.00730295	19					

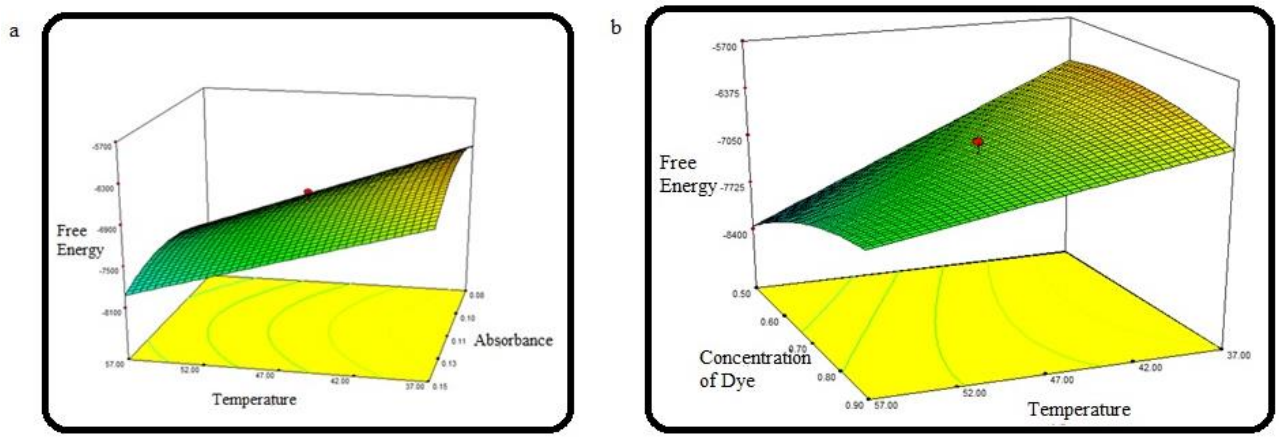

Fig. 4. (a) Surface plots of free energy with respect to temperature and absorbance; (b) Surface plots of free energy with respect to temperature and concentration of dye.

Table 4. ANOVA for response surface reduced quadratic model free energy

	Sum of Squares	df	Mean Square	F Value	Percent Contribution	p-Value Prob > F	Remarks
Model	9665926.6	9	1073992	54.49635		< 0.0001	Significant
t	6666539.9	1	6666540	338.2727	67.59	< 0.0001	
b	7064.4328	1	7064.433	0.358463	0.07	0.5627	
c	471109.56	1	471109.6	23.90498	4.77	0.0006	
t×b	56146.005	1	56146	2.848953	0.56	0.1223	
t×c	799986	1	799986	40.59279	8.11	< 0.0001	
b×c	42369.605	1	42369.6	2.149913	0.42	0.1733	
t^2	675.29679	1	675.2968	0.034266	0.006	0.8568	
b^2	1272503.4	1	1272503	64.5692	12.90	< 0.0001	
c^2	468403.01	1	468403	23.76764	4.74	0.0006	
Residual	197075.91	10	19707.59		1.9		
Lack of Fit	159903.77	5	31980.75	4.301711		0.0676	Not significant
Pure Error	37172.135	5	7434.427				
Cor Total	9863002.5	19					

Table 5. Optimization of process parameters for desirability

Temperature	Absorbance	Conc.	% Removal of dye	Ads. Capacity	Free energy	Desirability	Selection
55.9	0.08	0.6	93.38667	0.965	-8202.7	0.95082	Selected
56.1	0.08	0.59	93.33397	0.965	-8240.9	0.94917	
55.5	0.08	0.61	93.4876	0.965	-8123.6	0.93274	
55.9	0.08	0.6	93.38955	0.965	-8191.5	0.92983	
55.6	0.08	0.59	93.37901	0.965863	-8194.5	0.92396	
56.7	0.08	0.59	93.28879	0.963948	-8286.1	0.899312	

RSM modeling for free energy

Free energy modeling was performed using CCD to investigate the effect of the independent variables on free energy. Table 4 represents the design matrix and corresponding predicted results for free energy. A polynomial model was developed for free use employing RSM as given in eq. (3):

$$\text{Free energy} = -2495.98 - 201.638 \times t + 36614.52 \times b - 1388.26 \times c + 239.35 \times t \times b + 158.11\, t \times c + 10396.43\, b \times c - 0.06845\, t^2 - 242573\, b^2 - 4507.11\, c^2 \quad (3)$$

ANOVA results presented in Table 4 were used to evaluate the model. Fig. 4(a) shows a three-dimensional relationship between the temperature, absorbance, and concentration of dye with respect to free energy. Gibbs free energy increased with increase in temperature as reflected in Table 1 and RSM because the reaction is spontaneous and exergonic. Adsorption of dye is accompanied by decrease in the ΔG because the molecules of the adsorbate are held on surface of the solid adsorbent and as a result the entropy decreases. The experimental results and RSM prediction overlap quantitatively. On increasing the temperature from 27°C to 67°C dye mobility increases to a maximum value at corresponding temperature 55°C and dye concentration of 0.65 mg/L.

The variation between experimental and ANOVA predicted free energy is 0.99% and other statistic parameters of the ANOVA response surface reduced the quadratic model for free energy. The R^2 = 0.9800 of the free energy variable is well explained by the variance of the independent variable of the process. Similarly, Adj. R^2= 0.9620 satisfies the experimental curve, and Pred. R^2 = 0.8686 gives a satisfactory regression model under current constraints.

Optimization of process variables

The consistency and optimization of developed models was tested by performing confirmation experiments. The condition for the confirmation runs was set within the range of process parameters. The predicted value of performance variables was calculated from eqs. 1-3. Finally, the optimal values of the process, which maximize the process parameters of adsorption, were estimated from the desirability function of the RSM.

The calculated response was converted into desirability scale ranging from 0-1. The outcomes are represented in Table 5. It shows a maximum desirability 0.94 for a temperature range of 55.9-60.0 °C, concentration of dye 0.6 mg/L and percent removal of dye around 93.4 with constant absorbance of 0.08 a.u. The consistency and optimization of developed models was tested by performing confirmation experiments.

CONCLUSIONS

Response surface methodology - Central composite design (RSM-CCD) was successfully utilized as a statistical tool for optimizing free energy in dye removal from an aqueous solution by a bioadsorbent *Ricinus communis*. The highest percentage of CVD removal for experimental runs was 96 %, using 10 mg/L of adsorbent and a contact time of 2 hours. The correlation coefficient, R^2 for CVD removal in all ANOVA models, was found to be 0.9878. The optimum conditions for CVD removal, which were predicted by RSM, were found to be: temperature 55.9 °C, absorbance 0.08 a.u., initial concentration 0.6 mg/L, which resulted in maximum CVD removal of 93.38 % and minimized free energy 8202.7 J/mol at the desirability of 0.95.

REFERENCES

1. M. Dastkhoon, M. Ghaedi, A. Asfaram, H. Javadian, *Applied Organometallic Chemistry*, **32**(5), e4350 (2018).
2. M. R. Gadekar, M. M. Ahammed, *Journal of Environmental Management*, **231,** 241 (2019).
3. N. Arsalani, R. Nasiri, M, Zarei, *Chemical Engineering Research and Design*, **136,** 795 (2018).
4. A. M. Ealias, M. P. Saravanakumar, *Journal of Environmental Management*, **206,** 215 (2018).
5. J. Sharma, A. S. Chadha, V. Pruthi, P. Anand, J. Bhatia, B. S. Kaith, *Journal of Environmental Management*, **190,** 176 (2017).
6. R. R. Schio, N. P. G. Salau, E. S. Mallmann, G. L. Dotto, *Chemical Engineering Communications*, 1 (2020).
7. S. Debnath, K. Parashar, K. Pillay, *Carbohydrate polymers*, **175,** 509 (2017).
8. B. S. Kaith, U. Shanker, B. Gupta, J. K. Bhatia, *Reactive and Functional Polymers*, **131**, 107 (2018).
9. S. Karimifard, M. R. A. Moghaddam, *Science of the Total Environment*, **640,** 772 (2018).
10. M. Dastkhoon, M. Ghaedi, A. Asfaram, M. H. A. Azqhandi, M. K. Purkait, *Chemical Engineering Research and Design*, **124,** 222 (2017).
11. S. M. Pormazar, A. Dalvand, *International Journal of Environmental Analytical Chemistry*, 1 (2020).
12. M. M. Momeni, D. Kahforoushan, F. Abbasi, S. Ghanbarian, *Journal of Environmental Management*, **211**, 347 (2018).
13. L. A. Kafshgari, M. Ghorbani, A. Azizi, S. Agarwal, V. K. Gupta, *Journal of Molecular Liquids*, **233,** 370 (2017).
14. P. Banerjee, S. R. Barman, A. Mukhopadhayay, P. Das, *Chemical Engineering Research and Design*, **117,** 43 (2017).
15. A. Salehi, E. N. Kani, *Adsorption*, **4-7**, 647 (2018).
16. S., Karimifard, M. R. A. Moghaddam, *Process Safety and Environmental Protection*, **99,** 20 (2016).

17. A. K. Sharma, B. S. Kaith, V. Tanwar, J. K. Bhatia, N. Sharma, S. Bajaj, S. Panchal, *International Journal of Biological Macromolecules*, **129,** 214 (2019).
18. S. P. G. Zaferani, M. R. S. Emami, M. K. Amiri, E. Binaeian, *International Journal of Biological Macromolecules*, **139,** 307 (2019).
19. M. Khosravi, S. Arabi, *Water Science and Technology*, **74(**2), 343 (2016).
20. L. L. Melo, A. H. Ide, J. L. S. Duarte, C. L. P. Zanta, L. M. Oliveira, W. R. Pimentel Meili, *Environmental Science and Pollution Research International*, **27**(21), 27048 (2020).
21. A. Jawad, *Science Letters*, **14**(2), 1 (2020).
22. M. Iqbal, N. Iqbal, I. A. Bhatti, N. Ahmad, M. Zahid, *Ecological Engineering*, **88**, 265 (2016).
23. A. Mahajan, V. K. Sohpal, V. K. Bulasara, *Journal of Chemical Technology & Metallurgy*, **54**(1), 111 (2019).